Electronic structure and Fermi surfaces of transition metal carbides with rocksalt structure

2008 J. Phys.: Condens. Matter 20 225014

(http://iopscience.iop.org/0953-8984/20/22/225014)

J. Phys.: Condens. Matter **20** (2008) 225014 (6pp) doi:10.1088/0953-8984/20/22/225014

Electronic structure and Fermi surfaces of transition metal carbides with rocksalt structure

C Paduani

Departamento de Física, Universidade Federal de Santa Catarina, 88040-900, Florianópolis, SC, Brazil

E-mail: paduani@fisica.ufsc.br

Received 5 December 2007, in final form 14 April 2008
Published 15 May 2008
Online at stacks.iop.org/JPhysCM/20/225014

Abstract

First-principles calculations were carried out to investigate the structural and electronic properties of the metal carbides FeC, CoC, NiC, and PtC in the rocksalt structure. The full-potential linearized augmented-plane wave (FP-LAPW) method was used in the framework of the density-functional theory with the generalized gradient approximation (GGA) for the exchange–correlation potential. Ground state properties are determined and compared with available experimental data. The energy band structures, densities of states, and Fermi surface structures are obtained, which show that these compounds are metallic like the conventional transition metal carbides. There is an extensive hybridization between the metal-d and C-2p states for all the studied carbides, which can form bonding and antibonding states. From FeC to PtC a band narrowing for the hybridized metal-d and C-2p states near to the Fermi level takes place, which is expected to lead to smaller interactions between adjacent atoms. The largest bulk modulus of FeC is expected to be associated with the behavior of valence electrons near the Fermi level, i.e. a higher degree of hybridization between p–d states that are responsible for the chemical bonding results in strengthened interactions. The decrease in the number of bonding orbitals or decrease in metallic valence with the increase in number of 3d electrons from FeC to PtC provides a mechanism for weaker interactions due to the filling of antibonding bands.

(Some figures in this article are in colour only in the electronic version)

1. Introduction

Although transition metal nitrides have been considerably investigated both experimentally and theoretically, the amount of work which has been devoted to the transition metal carbides is only modest. The work on noble metal carbides is even more scarce. The interest in these compounds is due to their widespread use in industrial applications because of their remarkable physical, chemical, and mechanical properties. Some carbides have outstanding physical properties, such as high stiffness, high hardness, high thermal conductivity, and high melting points, which are desirable properties of good candidates for hard materials. The transition metal carbide molecules particularly provide an interesting and important set of diatomic molecules for experimental and theoretical study and represent a very active field of research, partly due to their relationship to catalytic reactions, but especially due to the significance of the transition metal–carbon bond in homogeneous and heterogeneous catalysis, biological processes, and organometallic chemistry. Nevertheless, among the transition metal carbides, the 4d series is by far the most completely studied. For the iron group carbides, in particular, theoretical and experimental information is still scarce. Several of the iron group carbides have recently been investigated in the gas phase by various research groups, and high level spectroscopic results are now available for the FeC molecules [1–3], CoC [4, 5] and NiC [6]. The 5d transition metal carbides otherwise represent a particular challenge to theoretical chemistry because of the simultaneous importance of relativistic, electron correlation, and spin–orbit effects.

The noble metal carbides are difficult to synthesize in crystal, and some of them were only observed in a metastable state. The earlier studies were focused on the transition metal carbides of group IV and group V. An analysis of

Table 1. Calculated lattice constants, bulk moduli, total DOS at the Fermi level ($N(E_F)$) and Fermi energy (E_F).

	Lattice constant (bohr)	B (GPa)	$N(E_F)$ ($\frac{\text{states}}{\text{Ryd.cell}}$)	E_F (Ryd)
FeC	7.4489	379.77	7.48	0.883 25
CoC	7.6121	319.16	21.50	0.764 75
NiC	7.3584	367.25	13.21	0.892 47
PtC	8.4608	261.38	15.78	0.846 71

the correlation between the cohesive energy and the average number of valence electrons per atom revealed striking regularities in these compounds. The bulk modulus in these carbides was found to be related to the number of valence electrons, through the filling of bonding p–d hybridized states [7, 8]. Recently the platinum carbide PtC has been synthesized at high pressure and high temperature by Ono *et al* [9] with the laser-heated diamond anvil cell technique. In their report, PtC has a rocksalt (RS) structure with a bulk modulus of 301(±15) GPa. However, a first-principles calculation performed by Li *et al* reported that RS-PtC is mechanically unstable, and that the zinc-blende (ZB) structure is preferred as more stable [10]. However, recent total energy calculations performed by Fan *et al* [11] on the elastic stability of PtC have indicated that this compound crystallizes into the RS structure, although this is metastable.

An analysis of the electronic band structure and valence charge distribution is useful for an understanding of the bonding mechanism in the carbides. The metal–nonmetal covalent bonding is important for understanding the physical properties of these compounds. The electronic band structure is determined by the shape of the Fermi surfaces (FS) which often results in a variety of ordering phenomena in metals and is intimately involved in the transport coefficients of a metal as well as in equilibrium and optical properties. In this contribution the electronic structure of the FeC, CoC, NiC, and PtC carbides is studied by means of scalar relativistic FP-LAPW calculations with the GGA approximation. Band structures and Fermi surfaces are calculated at the equilibrium lattice parameter, as obtained by a minimization of the binding energy against unit cell volume. The Fermi surfaces are presented in order to be compared with future experiments. The topology of FS plays a crucial role in determining the interactions and its study is worthwhile as it could help to provide a description of the metal–nonmetal interactions and bonding mechanism in the transition metal carbides. Generally a good agreement between theoretical and experimental trends is obtained.

2. Method

The calculations for these carbides in the rocksalt B1-type structure (space group 225—$Fm\bar{3}m$) were performed with the FP-LAPW plus local orbitals (APW + lo) method [12] within the framework of the density-functional theory with the generalized gradient approximation (GGA), where the Perdew–Burke–Ernzerhof (1996) parametrization was adopted for the exchange–correlation potential [13]. The approach

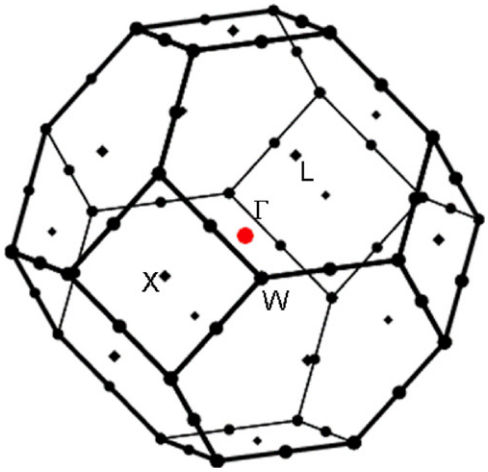

Figure 1. Primitive fcc Brillouin zone and symmetry points.

APW + lo, which reproduces the accurate results of the LAPW method using a smaller basis set, expands the wavefunctions of Kohn–Sham orbitals in spherical harmonics into atom-like orbitals inside the non-overlapping muffin-tin (MT) spheres, while in the interstitial region they are expanded in plane waves. This procedure is more suitable for calculations with a large ratio of basis functions to atoms. Additional local orbitals (LOs) were added to the basis sets for semi-core states to improve the variational flexibility. Muffin-tin sphere radii (R_{MT}) of 2.1 and 1.6 bohr were used for the transition metal and C atoms, respectively. The valence wavefunctions inside the MT spheres were expanded into spherical harmonics up to $l_{max} = 10$ and the $R_{MT} \times K_{max}$ was taken to be 7.0. 6000 k points were used for the integration procedure in the Brillouin zone by employing the improved tetrahedron method [16]. An energy criterion of convergence of 0.0 mRyd was chosen for the self-consistent cycles. The calculations were performed at the equilibrium lattice constants which were determined from a plot of the total energy against the unit cell volume by fitting to the Murnaghan equation of state [17].

3. Results and discussion

Figure 1 shows the primitive Brillouin zone of the fcc structure and some special symmetry points. In table 1 are listed the calculated equilibrium lattice constants for these carbides. Earlier estimated results are 7.72, 7.76, and 7.54 in bohr radii, for FeC, CoC, and NiC, respectively [8]. For PtC, the reported calculated value obtained by using the same approximation for the exchange–correlation potential (GGA) is 4.506 Å (8.515 bohr) [11]. In the present work 8.4608 bohr (4.477 Å) is obtained. The experimental value for PtC is 4.814 Å (9.097 bohr) [9]. As can be seen in table 1, the best agreement between the results of the present calculations with previously reported values for the equilibrium lattice constant are for CoC and PtC. Larger discrepancies are observed for FeC and NiC, as compared with earlier predictions. However, since the reported values for these are a rough estimate, the present results can be taken as a first report of calculated ground state properties. The calculated bulk moduli of these carbides are

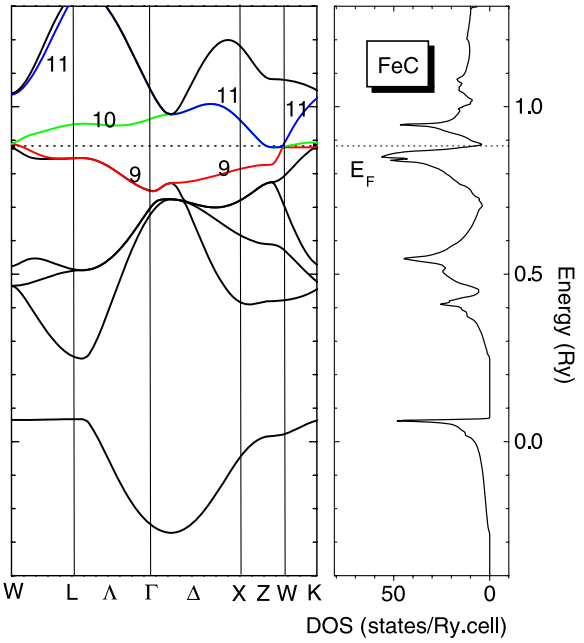

Figure 2. Left: band structure of FeC along symmetry directions around the Fermi level (dashed line) in the rocksalt (RS) structure; right: total DOS.

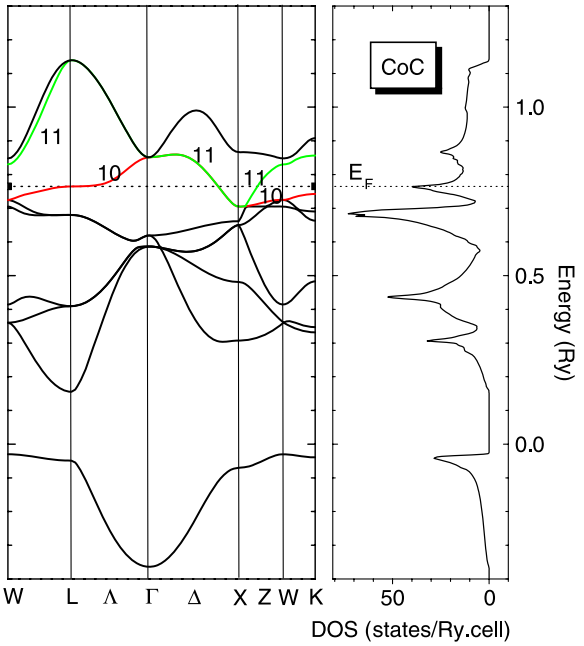

Figure 3. Band structure and total DOS of RS-CoC.

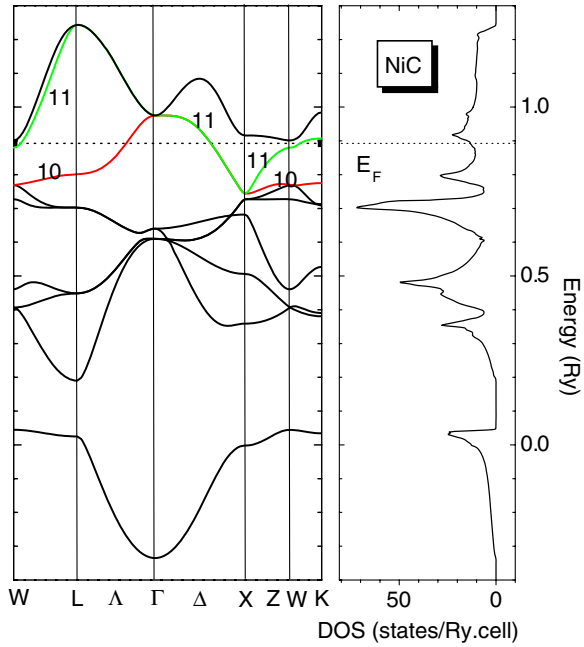

Figure 4. Band structure and total DOS of RS-NiC.

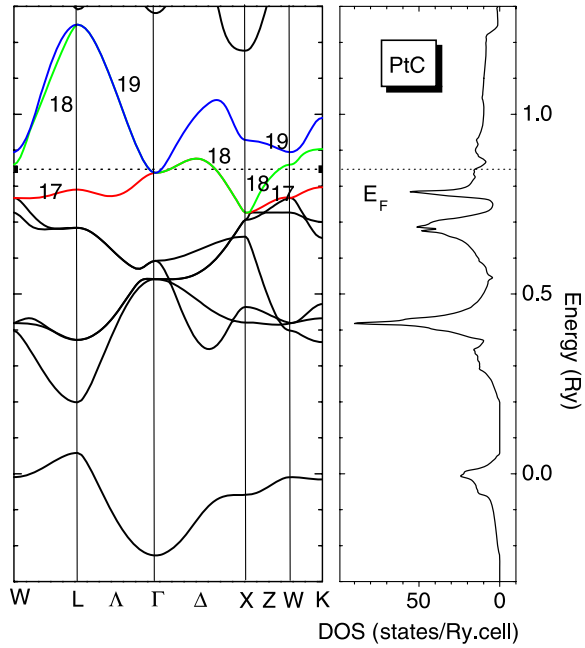

Figure 5. Band structure and total DOS of RS-PtC.

also listed in table 1. Interestingly enough, the 3d carbides possess even larger values of the bulk modulus than PtC, FeC having the largest one. However, it is noteworthy that the calculated result of the bulk modulus for PtC agrees well with the reported values in the literature [10, 11]. Unfortunately, for the 3d carbides there are no available experimental data of this quantity for comparison.

The densities of states at the Fermi level $N(E_F)$ are also included in table 1. Although few discrepancies exist between the present results and earlier reported results for the 3d carbides [8], generally the same trends are observed. For PtC, the DOS shown in figure 5 is in good agreement with the results of Fan *et al* [11]. CoC has the largest $N(E_F)$ value, followed by NiC and FeC, in a relative proportion of ≈3:2:1. The Fermi energies E_F shown in table 1 do not differ too much for FeC and NiC, which are higher than that of CoC, which has the smallest E_F value among these compounds. In figures 2–4 are shown the band structure plots and total densities of states (DOSs) for all the studied compounds. For FeC, in figure 2 one can see the formation of a gap of $\gtrsim$0.2 Ryd, which separates

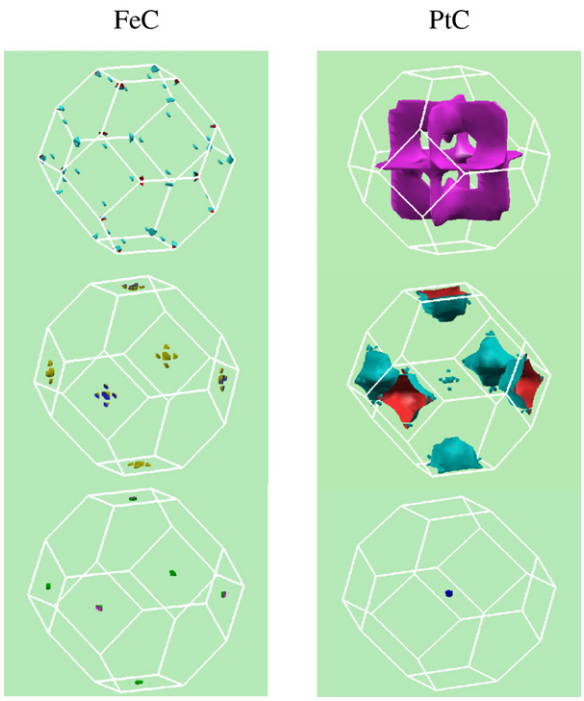

Figure 6. 3D plots of the Fermi surfaces from bands which cross the Fermi level. Left: FS from bands 9 (hole pockets) and 10–11 (electron pockets) for FeC; right: (left) FS from bands 17 (electrons), 18 (electron pockets centered at X and tiny hole pockets centered around Γ), and 19 (electron pocket) for PtC.

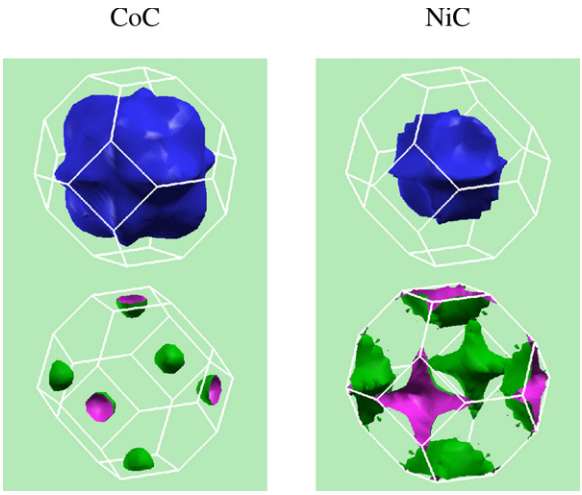

Figure 7. Fermi surfaces from bands 10 (hole pockets) and 11 (electron pockets) for both CoC (left) and NiC (right).

the low-lying s-states from the higher energy p-states. The peak in the DOS near 0.07 Ryd consists primarily of C s-states, whereas the DOS around the Fermi level is dominated by the Fe d-states. In FeC, the Fermi level lies near a minimum, which then yields a low $N(E_F)$ value. The high peak just below E_F is formed by Fe d-states which are gathered around L and W points of the irreducible Brillouin zone (IBZ); the peaks observed at 0.4–0.6 Ryd arise from bands which cross the Δ direction and are near to W points.

The additional d-electron of Co leads to a shift of the center of gravity of the total DOS towards lower energies, as can be seen in the diagram of figure 3. The Fermi level lies at a prominent peak, with the characteristic of a van Hove singularity. This is formed mainly by Co d-states from band 10, which appear flattened around L points in the IBZ; some contribution arises also from states close to the X points. The most prominent peak, observed at 0.6–0.7 Ryd, is primarily due to Co d-states around W points. The semi-core C s-states are localized at lower energies, as compared to FeC, whereas the C p-states yield their largest contribution within the energy range 0.35–0.55 Ryd. Another feature depicted in the diagram of figure 3 is a tendency for the accumulation of states around the zone center. For NiC, as one can see in figure 4, with the shift of the center of gravity of the DOS towards lower energies, the density of states at E_F decreases. Moreover, an increase in the number of degenerated bands is verified. The same trends are also observed for PtC, as seen in figure 5, where degenerated bands are crossing the Fermi level in the zone center. An accumulation of Pt d-states at the X and W points is observed. As a result, the highest peak in the DOS plot appears in the energy range 0.35–0.5 Ryd; the Fermi level lies in a shoulder of a small peak. From the DOS plots shown in figures 2–4 one is led to think that a rigid-band model is applicable to these compounds.

The calculated Fermi surface (FS) structures from bands which cross E_F for the studied compounds are shown in figures 6 and 7, which were obtained by using the Xcrysden code [18]. From top to bottom in figure 6 are shown the three-dimensional (3D) FS structure plots from bands 9 (hole pockets) and 10–11 (electron pockets) for FeC (left), and from bands 17 (electron pockets), 18 (electron sheets centered at X and hole sheets centered around Γ), and 19 (electron pockets) for PtC (right). As seen in the diagrams of figure 2 for FeC, few bands are crossing the Fermi level, which falls near a minimum of the DOS. This feature is also depicted in the FS of figure 6, which shows for band 9 tiny nodules being formed as hole pockets around W points and near the V direction. The FS from bands 10–11 for FeC, which are drawn as electron sheets, consist of an accumulation of five small open shells forming electron pockets around X points. The energy ranges for these bands are 0.74–0.89 Ryd for band 9, 0.87–1.02 Ryd for band 10, and 0.87–1.34 Ryd for band 11 of FeC. Hence, if one lowers E_F by a few mRyd the contributions from these two bands disappear, while if E_F is raised slightly by only a few mRyd the contribution from band 9 disappears.

The FS 3D plots for PtC are shown on the right in figure 6. For band 17, which is drawn as a hole sheet, one sees a structure of hole pockets which resembles ‘three thick squares each one with four circular holes’ and which are interpenetrated orthogonally and centered in the zone center (Γ). Its energy range spans from about 0.72 Ryd up to 0.87 Ryd. For band 18, a sort of ‘thick star-fish’ is seen for the electron pockets centered around X points, as well as a few small globules of hole pockets that can be seen gathered around the zone center. Hence, both kind of charge carriers, i.e. holes and electrons, are present. The energy range is 0.73–1.25 Ryd. For band 19, a single nodule of an electron pocket is seen in

the zone center, a feature which is also clearly identified in the band plot of figure 5; the energy range for this band is 0.83–1.25 Ryd.

In figure 7 are shown the FS structure 3D plots from bands crossing E_F for CoC and NiC, where one can see similar features for both the compounds. Only two bands are crossing E_F, namely, bands 10 (hole pockets) and 11 (electron pockets). The energy ranges are 0.70–0.86 Ryd and 0.70–1.14 Ryd for band 10 of CoC and NiC, respectively. For band 11, the energy ranges for CoC and NiC are 0.73–0.97 Ryd and 0.74–1.25 Ryd, respectively. The FS structures of hole pockets from bands 10 for CoC and NiC resemble the structure of interpenetrating squares, as shown in figure 6 for band 17 of PtC, although in this case they look much thicker and 'inflated', particularly for CoC, and are fulfilling a larger portion of the Brillouin zone. On the other hand, the electron pockets from band 11 for this carbide consist of semi-spherical bosses, whereas for NiC it forms a structure which resembles a 'thick star-fish', and in both cases, centered at the X points of the IBZ. As one goes throughout this series, from FeC to NiC, one sees that E_F initially decreases and after that increases, with an increase in the number of 3d electrons, and the filling of the valence bands therein leads to the shift of the Fermi level towards a resonance in the DOS, an effect which causes major changes at the zone boundary, specially around L and X points.

The bulk modulus in the transition metal carbides is related to the number of valence electrons which are the bonding electrons. Hence, the distribution of valence electrons close to the Fermi level and the hybridization between p-and d-states is determined for the cohesion properties. From FeC to PtC, the shift toward lower energies of the center of gravity of the DOS causes a reduction in the degree of hybridization of the valence states between metal and nonmetal, which in turn, leads to a band narrowing which results in a weakening of the interactions. As a consequence, the bulk modulus decreases. Furthermore, by inspecting the band structure plots of FeC, CoC and NiC, one is led to think that the main feature responsible for the largest value of the bulk modulus of FeC, as compared to the others, is the fact that the valence band 9 is almost completely filled up, whereas band 10 is in its largest extension above E_F, conversely to the observed behavior in the other carbides. The bonding band being filled contributes to an increase in the cohesive energy, as observed for FeC, where band 9 is almost entirely below E_F. Moreover, from the band structure plots one observes a tendency to form degenerate bands around W points, from FeC to PtC, an effect which might be contributing to the decrease in the bulk modulus, as a result of weakened interactions. A smaller overlap of the valence bands is observed for FeC on the X points. Furthermore, from the band structure plots it is observed that there is an extensive hybridization between the metal-d and C-2p states for all the studied carbides, which forms bonding and antibonding states. As one goes from FeC to PtC a band narrowing for the hybridized metal-d and C-2p states near the Fermi level is taking place, which is expected to lead to weaker interactions between orbitals on adjacent atoms. The decrease in number of bonding orbitals or decrease in metallic valence with the increase in number of d electrons also provides a mechanism for weaker interactions, due to the filling of antibonding bands. Going from CoC to PtC, it is seen that the connectivity of bands which contribute to the bonding character (net reinforcement) takes place around X points, around which the electron pockets are gathered, which determines the nature of the bonds between metal and nonmetal.

As far as transport properties are concerned, striking differences are observed between these compounds. For FeC, the low density of states $N(E_F)$ at E_F indicates that the low temperature state of this material is a very poor metal. From the FS plots in figure 6 one sees also that the carriers are almost localized. For PtC, the presence of both carriers (electrons and holes) indicates that rather complex galvanometric properties are expected. Moreover, the Fermi surface peculiarities around X points indicate a propensity for nesting instabilities (superposition of electron–hole pockets). For CoC, where a van Hove singularity is identified at E_F, the hole states occupy a large portion of the IBZ volume. The increased hybridization acts in a sense to increase $N(E_F)$. From figure 7 it is seen that, for NiC, similarly to CoC, the FS is composed of a hole pocket around the zone center and large electron pockets around X points, thus meaning that the behavior of surface state carriers is electron-like. The existence of the electron pockets at X points in the IBZ for these compounds indicates a negative Hall coefficient R_H (the most natural explanation for the negative R_H is the presence of an electron pocket in the Fermi surface). When the FS contains both electron and hole pockets, the sign of R_H depends on the relative magnitude of the respective electron–hole densities and mobilities. Nevertheless a common feature observed from the band structure and FS plots is that a metallic behavior can be inferred for all the studied carbides.

4. Conclusion

The ground state properties of the carbides FeC, CoC, NiC and PtC were investigated in the rocksalt structure by first-principle calculations. The results indicate a metallic behavior for these compounds. The calculated bulk modulus is the highest for FeC, followed by NiC, CoC, and PtC. From a comparison of the band structure and Fermi surface plots for these carbides one concludes that this behavior is directly related to the hybridization of the p–d valence states near E_F. With the increase in the number of d electrons from FeC to PtC the decrease in number of bonding orbitals or decrease in metallic valence provides a mechanism for weaker interactions due to the start of the filling of antibonding bands. The calculations show that the Fermi surfaces of these carbides are extremely sensitive to small shifts in the relative positions of the bands. The electronic structures of these compounds are strongly determined by the metal-d and C-2p interaction and thereby the topology of the Fermi surface is strongly affected by the large hybridization between these bands.

Acknowledgments

The authors would like to thank the Brazilian Agencies CNPq and Finep.

References

[1] Balfour W J, Cao J, Prasad C V V and Qian C X W 1995 *J. Chem. Phys.* **103** 4046

[2] Allen M D, Pesch T C and Ziurys L M 1996 *Astrophys. J.* **472** L57

[3] Brugh D J and Morse M D 1998 *J. Chem. Phys.* **107** 9772

[4] Barnes M, Merer A J and Metha G F 1995 *J. Chem. Phys.* **103** 8360

[5] Adams A G and Peers J R D 1997 *J. Mol. Spectrosc.* **181** 24

[6] Brugh D J and Morse M D 2002 *J. Chem. Phys.* **117** 10703

[7] Guillermet A F and Grimvall G 1989 *Phys. Rev.* B **40** 10582

[8] Häglund J, Grimvall G, Jarlborg T and Guillermet A F 1991 *Phys. Rev.* B **43** 14400

[9] Ono S, Kikegawa T and Ohishi Y 2005 *Solid State Commun.* **133** 55

[10] Li L Y, Yu W and Jin C Q 2005 *J. Phys.: Condens. Matter* **17** 5965

[11] Fan C Z, Sun L L, Wang Y X, Liu R P, Zeng S Y and Wang W K 2006 *Physica* B **381** 174
Fan C Z, Zeng S Y, Zhan Z J, Liu R P, Wang W K, Zhang P and Yao Y G 2006 *Appl. Phys. Lett.* **89** 071913

[12] Blaha P, Schwarz K, Madsen G K H, Kvasnicka D and Luitz J 2002 A full-potential linearized augmented-plane wave package for calculating crystal properties *WIEN2k* Vienna University of Technology
Schwarz K, Sorantin P and Trickey S B 1990 *Comput. Phys. Commun.* **59** 399
Schwarz K, Blaha P and Madsen G K H 2002 *Comput. Phys. Commun.* **147** 71

[13] Perdew J P, Burke S and Ernzerhof M 1996 *Phys. Rev. Lett.* **77** 3865

[14] Koelling D D and Harmon B N 1977 *J. Phys. C: Solid State Phys.* **10** 3107

[15] Desclaux J P 1969 *Comput. Phys. Commun.* **1** 216
Desclaux J P 1975 *Comput. Phys. Commun.* **9** 31

[16] Blochl P E, Jepsen O and Andersen O K 1994 *Phys. Rev.* B **49** 16223

[17] Murnaghan F D 1944 *Proc. Natl Acad. Sci. USA* **30** 244

[18] Kokalj A 1999 *J. Mol. Graph. Modelling* **176** 17